COMPUTATIONAL MECHANICS
New Trends and Applications
S. Idelsohn, E. Oñate and E. Dvorkin (Eds.)

AN UNSTRUCTURED FINITE VOLUME PROCEDURE FOR SIMULATING FLOWS WITH MOVING FRONTS

Maliska, C. R.*and Vasconcellos, J. F. V.†

SINMEC - Computational Fluid Dynamics Laboratory
Mechanical Engineering Department - UFSC - P.O. Box 476
88040-900 - Florianópolis - SC - Brazil
web page: http://www.sinmec.ufsc.br/
*e-mail: maliska@sinmec.ufsc.br
†e-mail: jflavio@sinmec.ufsc.br

Key words: Finite Volume Method, Voronoi Diagram, Unstructured Grids, Computational Fluid Dynamics

Abstract *The correct prediction of moving fronts is of utmost importance in mold injection. Due to the complexity of the computational domains encountered in this engineering application, finite element methods are widely used for predicting the fluid flow. The prediction of the position of the front are, however, usually done using finite-differences because of local mass conservation requirements. This paper presents a finite volume method for simulating flows with moving fronts using Voronoi discretization, where the conservation principles are obeyed in solving the flow variables inside the domain as well as in the moving front. The method extends the knowledge of the classical finite volume method for structured grids to unstructured grids.*

1 INTRODUCTION

Mold filling injection and casting are widely used procedures for manufacturing and production of plastic and metal parts. The ability to simulate the filling process realistically allows the engineer to optimize the mold design. The flow in mold injection presents an important characteristic: the existence of a continuously moving boundary whose location is not known *a priori*. Therefore, modelling such flows is a challenging task, since the free surface profile is continuously moving and the correct prediction of the front position depends on the correct application of the boundary conditions at the front. The algorithms for predicting fluid flows inside mold cavities can be divided in two broad categories according to the gridding: grids which adapts to the moving fronts (Lagrangian methods) and fixed grids. The methods in the former category do not have the difficult in calculating the volume which is occupied by the filling fluid in the computational cell at the moving front. However, the remeshing can be costly. The methods in the latter category just lay down a mesh over the whole domain and solve the governing equation for both fluids (filling fluid and air, for example) keeping track of the void fraction at the moving front. The methods can be also explicit or implicit, being the former ones limited by stability characteristics given by the Courant number. This limitation becomes increasingly restrictive with mesh refinement. Pioneering explicit methods for predicting moving fronts are the well known MAC method of Welch *et alii*[1] and its variants of Hwang and Stoher[2,3], the GENSMAC of Thome and McKee[4] among others and the VOF technique of Hirt and Nichols[5]. The idea of the VOF method has been applied in several situations with success. Implementation of the VOF method in a finite element framework was recently done by Dhatt *et alii*[6] and Usmani *et alii*[7]. The basic idea behind VOF is to solve a new partial differential equation for the volume of the fluid in the computational cell. A value of this variable equal to zero indicates that the cell is empty, equal to one, a full cell, and between zero and one, a partially filled cell. Swaminathan and Voller[8] presented a time-implicit filling algorithm which uses the VOF ideas and avoids the liming Courant number of explicit schemes.

This paper presents a finite-volume method using unstructured grids of Voronoi type for the solution of fluid flows in mold cavities. The moving front is modelled using the ideas of the VOF method presented in [8], while the field equations are solved using an unstructured finite-volume method (UFVM) proposed in [14] and implemented in [15], which is an extension of the classical finite-volume method for structured grids. The paper presents results for two and three-dimensional flows in mold cavities. The 3D grid is obtained by repeating the 2D grid in the z-direction. This is adequate because mold cavities are usually thin and the procedure to generate the grid is, therefore, straightforward.

2 THE VOF METHOD

In the VOF method there is the addition of one partial differential equation for the volume fraction (F) of the computational cell, given by

$$\frac{\partial}{\partial t}(\rho_l F) + \nabla \cdot (\rho_l \vec{V} G) = 0 \tag{1}$$

where F is the liquid fraction and is related to G through

$$\begin{aligned} &\text{if} \quad F < 1 \quad \text{then} \quad G = 0 \\ &\text{if} \quad F = 1 \quad \text{then} \quad G > 0 \end{aligned} \tag{2}$$

As clearly described in [8], Eq. 1, which for filling process is merely an auxiliary equation to calculate the fractional volume of the cell, is analogous to the equation which governs phase-change phenomena. The characteristic of the equation in this case is that the cell does not change its temperature and do not looses heat while it is undergoing a phase change. In the filling process, this means that while the cell is filling there is no fluid flow at the cell boundaries. Inspecting Eq. 1 one realizes that the second term is a convective one, therefore, susceptible to numerical diffusion if the fluxes at the interfaces are not proper evaluated. The procedure adopted in [8] is applied in this work.

Another important characteristic of the VOF method concerns to the solution of the corresponding Navier-Stokes equation. While other methods uses Eq. 1 but solves the Navier-Stokes equation for the liquid region only, the VOF method solves this equation for the whole domain (liquid and gas), which resembles the solution of a single-phase flow. The Navier-Stokes and mass conservation equations for the "single-phase flow" are given by

$$\frac{\partial}{\partial t}(\rho_F \vec{V}) + (\rho_G \vec{V} \cdot \nabla)\vec{V} = -\nabla p + \nabla \cdot (\mu_G \nabla \vec{V}) + \vec{f}_F \tag{3}$$

$$\nabla \cdot \vec{V} = 0 \tag{4}$$

where constant density for the liquid and gas phases are assumed and the volume-averaged properties are given by

$$\begin{aligned} \rho_F &= F\rho_l + (1 - F)\rho_g \\ \mu_G &= G\mu_l + (1 - G)\mu_g \end{aligned} \tag{5}$$

where ρ_l and μ_l are the density and the viscosity for the liquid and ρ_g and μ_g are the density and the viscosity for the gas. Details of how to calculate the interface fluxes can be found in [8].

In this work the momentum equation is not simplified to the usual form used in mold filling, where the nonlinear terms are neglected. The full Navier-Stokes equation is maintained, therefore the algorithm can be applied to general filling processes.

3 NUMERICAL PROCEDURE

Eqs. (3) and (4) are the flow equations, represented by the momentum and the mass conservation equations, and Eq. (1) is the so-called filling equation. The complexity of the equation set and of the shape of real mold cavities, precludes the determination of analytical solutions. Even finite-volume methods based on boundary-fitted coordinates encounter difficulties in being applied because it is not easy to find a global coordinate system which maps complex cavities onto a single rectangle for bi-dimensional cases or hexahedron for three-dimensional cases. Finite Element Methods (FEM) are widely used in mold filling processes, specially when the inertia terms are neglected and the resulting equation can be solved using the standard Galerkin approximation[9]. Another route using unstructured grids is the use of the Control Volume Finite Element approach (CVFEM), in which the conservation principles are obeyed and the interpolation procedures has some similarities with the classical FEM[10]. In this paper a new approach is presented, where the well known methodologies used in finite-volume methods for structured grids are extended to unstructured grids of Voronoi type, keeping the strong physical appealing inherent to finite-volume methods.

The use of Voronoi grids render to the method the important property of local orthogonality where, for isotropic flows, this means that the flow driving force is always orthogonal to the control volume surface. This condition simplifies considerably the numerical implementation.

There are only few methods for the solution of the full Navier-Stokes equation using Voronoi grids available in the literature. Among them the method of Taniguchi and Kobayashi[11] and Taniguchi *et alii*[12] presents an efficient method for calculating the pressure gradient in Voronoi diagrams. Davidson[13] also solved fluid flow problems using Voronoi grids, but with a more complex method for calculating the pressure gradient. The procedure for solving the momentum equation in the filling processes analyzed in this paper was presented in [14] and implemented and tested in [15]. In this paper this procedure in used in conjunction with the filling equation of the VOF method extended to unstructured grids.

The conservation equation written for a scalar ϕ in vector form is given by

$$\frac{\partial}{\partial t}(\rho_F \phi) = \nabla \cdot (\Gamma^{\phi} \nabla \phi - \rho_G \vec{V} \phi) + S^{\phi} \tag{6}$$

Table 1 shows the corresponding coefficients and source terms for the ϕ variables for three-dimensional problems, where u, v, w and p are the unknowns.

Table 1 - Values of ϕ, Γ^ϕ and S^ϕ

Equation	ϕ	$^\phi$	S^ϕ
Mass Conservation	1	0	0
Momentum Conservation - x direction	u	μ_G	$\frac{\partial}{\partial x}(\mu_G \frac{\partial u}{\partial x}) + \frac{\partial}{\partial y}(\mu_G \frac{\partial v}{\partial x}) + \frac{\partial}{\partial z}(\mu_G \frac{\partial w}{\partial x}) - \frac{\partial P}{\partial x}$
Momentum Conservation - y direction	v	μ_G	$\frac{\partial}{\partial y}(\mu_G \frac{\partial v}{\partial y}) + \frac{\partial}{\partial x}(\mu_G \frac{\partial u}{\partial y}) + \frac{\partial}{\partial z}(\mu_G \frac{\partial w}{\partial y}) - \frac{\partial P}{\partial y}$
Momentum Conservation - z direction	w	μ_G	$\frac{\partial}{\partial z}(\mu_G \frac{\partial w}{\partial z}) + \frac{\partial}{\partial x}(\mu_G \frac{\partial u}{\partial z}) + \frac{\partial}{\partial y}(\mu_G \frac{\partial v}{\partial z}) - \frac{\partial P}{\partial z}$

The basic step in the FVM is to integrate the conservation equations in divergence form over the control volume. Considering Fig. 1, where the control volume (Voronoi diagram) centered in P and their neighbours are depicted, the integration of Eq. (6) in time and over the control volume reads

$$\int_V \rho(\phi - \phi^o)dV = \int_t (\sum_i^N (J \cdot \Delta S)_i + S^\phi \Delta V)dt \tag{7}$$

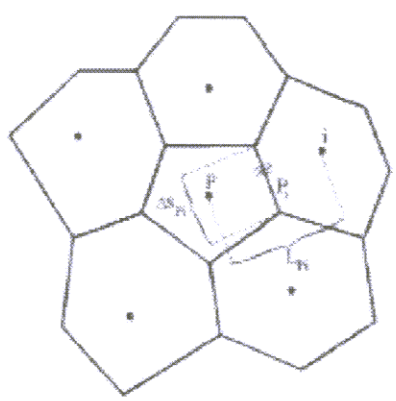

Figure 1. Control volume used to integrate Eq. (7)

Recalling the properties of the Voronoi diagram, each term of Eq. (7) can be integrated as

$$\int_V \rho(\phi - \phi^o)dV = M_P \phi_P - M_P^o \phi_P^o \tag{8}$$

where M_P is the mass in the volume P. The superscript o denotes that this variable is based on the previous time step. Integration of the first term in the right-hand side gives

$$\begin{aligned}\int_t \sum_i^N (J \cdot S)_i dt &= \int_t \sum_i^N ((\Gamma^\phi \nabla\phi - \rho_G \vec{V}\phi) \cdot S)_i dt \\ &= \left(\sum_i^N \Gamma \frac{\partial\phi}{\partial\vec{n}} \right)_{Pi} \Delta S_{Pi} - \sum_i^N \rho_G (\vec{V} \cdot \vec{n})_{Pi} \phi_{Pi} \Delta S_{Pi} \Bigg) \Delta t\end{aligned} \tag{9}$$

Eq. (7) then assumes the follow form

$$\begin{aligned}\frac{M_P\phi_P - M_P^o\phi_P^o}{\Delta t} &= \sum_i^N \Gamma \frac{\partial\phi}{\partial\vec{n}} \Bigg)_{Pi} \Delta S_{Pi} - \\ &\sum_i^N \rho_G (\vec{V} \cdot \vec{n})_{Pi} \phi_{Pi} \Delta S_{Pi} + (S_P\phi_P + S_c)\Delta V_P\end{aligned} \tag{10}$$

Eq. (10) reveals that the normal derivative of ϕ and the values of ϕ at the control volume interfaces must be calculated as functions of the grids values of ϕ. This procedure is the application of the interpolation function and is responsible for the order of approximation of the numerical scheme. High order interpolation functions will render to the method lower truncation errors but may introduce numerical oscillations. In the other hand, first order interpolation functions for the convective terms will introduce the undesirable numerical diffusion. In this paper the diffusion terms are evaluated using Central Differencing and the convective ones using the hybrid WUDS scheme[16]. Therefore, the normal derivative, $\left.\frac{\partial\phi}{\partial\vec{n}}\right|_{Pi}$, can be easily derived due to the local orthogonality of the Voronoi diagrams, by

$$\left.\frac{\partial\phi}{\partial\vec{n}}\right|_{Pi} = \frac{\phi_i - \phi_P}{L_{Pi}} \tag{11}$$

and the values of ϕ at the interfaces by

$$\phi_{Pi} = (\frac{1}{2} + \alpha_i)\phi_P + (\frac{1}{2} - \alpha_i)\phi_i \tag{12}$$

where α_{Pi} is calculated by

$$\alpha_{Pi} = \frac{P_e^2}{10 + 2P_e^2} \tag{13}$$

and the local Peclet number, Pe, is defined as

$$P_e = \frac{V_{Pi} L_{Pi}}{\Gamma^\phi} \tag{14}$$

where V_{Pi} is the normal velocity at interface i.

Using the above expressions, Eq. (7) can be rewritten as

$$\begin{aligned} &\phi_P \left\{ \frac{M_P}{\Delta t} + \sum_i \left(\frac{\Gamma^\phi_{Pi}}{L_{Pi}} + \rho_G V_{Pi} (\frac{1}{2} + \alpha_{Pi}) \right) \Delta S_{Pi} - S_P \Delta V \right\} = \\ &\phi_i \left\{ \sum_i \left(\frac{\Gamma^\phi_{Pi}}{L_{Pi}} - \rho_G V_{Pi} (\frac{1}{2} - \alpha_{Pi}) \right) \Delta S_{Pi} \right\} + \frac{M_P^o \phi_P^o}{\Delta t} + S_c \Delta V_P \end{aligned} \tag{15}$$

Eq. (15) is further simplified by introducing the mass conservation equation

$$-\sum_i \rho_G V_{Pi} \Delta S_{Pi} - \frac{M_P}{\Delta t} + \frac{M_P^o}{\Delta t} = 0 \tag{16}$$

resulting

$$\begin{aligned} &\phi_P \left\{ \sum_i \left(\frac{\Gamma^\phi_{Pi}}{L_{Pi}} - \rho_G V_{Pi} \left(\frac{1}{2} - \alpha_{Pi} \right) \right) \Delta S_{Pi} - S_P \Delta V_P + \frac{M_P^o}{\Delta t} \right\} = \\ &\left\{ \sum_i \left(\frac{\Gamma^\phi_{Pi}}{L_{Pi}} - \rho_G V_{Pi} \left(\frac{1}{2} - \alpha_{Pi} \right) \right) \Delta S_{Pi} \right\} \phi_i + \frac{M_P^o \phi_P^o}{\Delta t} + S_c \Delta V_P \end{aligned} \tag{17}$$

or simply

$$A_p \phi_P = \sum A_i \phi_i + B \tag{18}$$

where

$$A_i = \left\{ \frac{\Gamma^{\phi}_{Pi}}{L_{Pi}} - \rho_G V_{Pi} \left(\frac{1}{2} - \alpha_{Pi} \right) \right\} \Delta S_{Pi} \tag{19}$$

$$A_P = \sum A_i - S_P \Delta V_P + \frac{M^o_P}{\Delta t} \tag{20}$$

$$B = S_c \Delta V_P + \frac{M^o_P \phi^o_P}{\Delta t} \tag{21}$$

Eq. (18) can be solved using any available solver for linear system of equations. As already stated, this equation is valid for any scalar ϕ using the appropriate source term and diffusion coefficient. In this paper ϕ will assume the role of u and v Cartesian velocity components.

4 THE PRESSURE GRADIENT CALCULATION

The pressure gradient in the momentum equations are present in the source term of Eq. (18). This pressure gradient needs to be calculated at the center of the control volume for u and v. When structured grids are used this is a simply calculation since the grid points are along a coordinate line. For unstructured grids, considering the momentum equation for u, the calculation of $\partial p/\partial x$ is not straightforward. This is one of the key questions in solving the momentum equation for unstructured grids. The algorithm used herein is based on the minimization technique which involves the solution of a linear equation system for each volume, which was proposed by Taniguchi *et alii*[12] and can be seen in a detailed form in Cardoso[17].

For a 3D calculation the matrix for calculating the pressure gradient in each local coordinate directions is given by

$$\begin{bmatrix} \sum_i^N g^{Pi} e_{xi}^2 & \sum_i^N g^{Pi} e_{xi} e_{xi} & 0 \\ \sum_i^N g^{Pi} e_{xi} e_{xi} & \sum_i^N g^{Pi} e_{yi}^2 & 0 \\ 0 & 0 & \sum_i^N g^{Pi} e_{zi}^2 \end{bmatrix} \begin{bmatrix} \frac{\Delta p}{\Delta x} \\ \frac{\Delta p}{\Delta y} \\ \frac{\Delta p}{\Delta z} \end{bmatrix} = \begin{bmatrix} \sum_i^N g^{Pi} \nabla P_i e_{xi} \\ \sum_i^N g^{Pi} \nabla P_i e_{yi} \\ \sum_i^N g^{Pi} \nabla P_i e_{zi} \end{bmatrix} \tag{22}$$

where

$$g^{Pi} = \frac{\Delta S_{Pi}}{L_{Pi}}$$

$$\nabla P_i = \frac{P_i - P_P}{L_{Pi}} \tag{23}$$

and e_{xi}, e_{yi} and e_{zi} are the x, y and z components of the normal vector at the cell face i, respectively. The zeros appearing in the matrix in Eq. (22) is because the 3D grid is constructed by assembling layers of 2D Voronoi grids.

5 THE PRESSURE-VELOCITY COUPLING

The pressure-velocity coupling is handled using the well-known SIMPLEC algorithm[18]. This methodology, which obtain velocity and pressure fields satisfying the conservation laws simultaneously, was originally proposed to be used with structured grids. Maliska[14] introduced a method, base on SIMPLEC, to be used with unstructured grids. In this procedure it is required to create a correction equation for the velocity components. It is proposed that the normal velocity , V_{Pi}, at each cell-face is corrected by the relation

$$V_{Pi} = V^*_{Pi} - \frac{(P'_P - P'_i)}{\overline{(A_P - \sum A_{nb})_{Pi}}} \frac{\overline{\Delta V}}{L_{Pi}} \tag{24}$$

where P' is the pressure correction which is related to the pressure P according to

$$P = P^* + P' \tag{25}$$

and P^* is the estimated pressure field. Since there is no central nor connecting coefficients at the interfaces, the term $A_P - \sum A_{nb}$ is calculated using the coefficients of the neighbouring central volumes according to the geometric interpolation proposed in Vasconcellos and Maliska[6]

$$\overline{(A_P - \sum A_{nb})_{Pi}} = \frac{2(A_P - \sum A_{nb})_P (A_P - \sum A_{nb})_i}{(A_P - \sum A_{nb})_P + (A_P - \sum A_{nb})_i} \tag{26}$$

Upon substituing Eq. (24) into the continuity equation, one obtains a Poisson equation for the pressure correction, as

$$A_p P'_P = \sum_i^N A_i P'_i + B \tag{27}$$

where

$$A_i = \frac{\overline{\Delta V}}{(\overline{A_P - \sum A_{nb}})_{Pi}} \frac{\Delta S_{Pi}}{L_{Pi}} \tag{28}$$

$$A_P = \sum_i^N A_i \tag{29}$$

$$B = \sum_i^N V^*_{Pi} \Delta S_{Pi} \tag{30}$$

6 VELOCITY AT THE INTERFACES

Since this method uses co-located variables and the velocities u, v and w are required at the interfaces of the control volume, interpolation should be done to find these velocities. This works extends the interpolation technique proposed in Marchi and Maliska[19] to be used with unstructured grids, whereby an interpolation of the momentum equations are realized instead of only interpolating the calculated quantities.

The u^*, v^* and w^* velocities at the cell-faces are, therefore, given by

$$u^*_{Pi} = \frac{\sum(A_{NB}u^*_{NB})_P + \sum(A_{NB}u^*_{NB})_i + (Sc\Delta V)_P + (Sc\Delta V)_i}{(A_P)_P + (A_P)_i} + \frac{\frac{(M^o_P + M^o_i)}{\Delta t} u^o_{Pi} - (2\frac{\Delta P}{\Delta x})_{Pi}\overline{\Delta V}}{(A_P)_P + (A_P)_i} \tag{31}$$

$$v^*_{Pi} = \frac{\sum(A_{NB}v^*_{NB})_P + \sum(A_{NB}v^*_{NB})_i + (Sc\Delta V)_P + (Sc\Delta V)_i}{(A_P)_P + (A_P)_i} + \frac{\frac{(M^o_P + M^o_i)}{\Delta t} v^o_{Pi} - (2\frac{\Delta P}{\Delta y})_{Pi}\overline{\Delta V}}{(A_P)_P + (A_P)_i} \tag{32}$$

$$w^*_{Pi} = \frac{\sum(A_{NB}w^*_{NB})_P + \sum(A_{NB}w^*_{NB})_i + (Sc\Delta V)_P + (Sc\Delta V)_i}{(A_P)_P + (A_P)_i} + \frac{\frac{(M^o_P + M^o_i)}{\Delta t} w^o_{Pi} - (2\frac{\Delta P}{\Delta z})_{Pi}\overline{\Delta V}}{(A_P)_P + (A_P)_i} \tag{33}$$

where

$$\overline{\Delta V} = \frac{[(\Delta V)_P + (\Delta V)_i]}{2} \tag{34}$$

Observe that the pressure gradient in these equation are evaluated at the interface and, in this case, they are easily available since pressure nodes are along the normal at the interface, a characteristic of the Voronoi diagrams.

7 APPLICATION OF THE FILLING EQUATION

Since this paper deals with the solution of the fluid flow in filling processes, it is now required the solution of the filling equation, which will give us the value of the variable F. This variable indicates the amount of each cell is filled with liquid. The method used in this work was developed by Swaminathan and Voller[8] for Cartesian coordinates.

The filling equation, Eq. (1) is integrated in time and over the control volume shown in Fig. 1, resulting in

$$\rho_l(F_p - F_P^o)\frac{\Delta V_p}{\Delta t} + \sum \rho_l V_{Pi} G_{Pi} \Delta S_{Pi} = 0 \tag{35}$$

Again it is recognized that the convective fluxes, involving the G variable, need to be evaluated at the interfaces. The interpolation adopted is based on the same hybrid scheme used for the momentum equation

$$G_{Pi} = \left(\frac{1}{2} + \alpha_i\right) G_P + \left(\frac{1}{2} - \alpha_i\right) G_i \tag{36}$$

where

$$\begin{aligned} \alpha_i &= 0.5 \qquad \text{if} \quad V_{Pi} > 0 \\ \alpha_i &= -0.5 \qquad \text{if} \quad V_{Pi} < 0 \end{aligned} \tag{37}$$

Eq. (35), after using the interpolation function can be rewritten as following

$$\rho_l(F_p - F_P^o)\frac{\Delta V_p}{\Delta t} + \sum \rho_l V_{Pi} \left((\frac{1}{2} + \alpha_i) G_P + (\frac{1}{2} - \alpha_i) G_i \right) \Delta S_{Pi} = 0 \tag{38}$$

For each control volume, Eq. (39), given below, is solved to determine the value of G

$$G_P = \frac{\rho_l(F_P^o - F_P)\frac{\Delta V_p}{\Delta t} - \sum \rho_l V_{Pi} \left(\frac{1}{2} - \alpha_i\right) G_i \Delta S_{Pi}}{\sum \rho_l V_{Pi} \left(\frac{1}{2} + \alpha_i\right) \Delta S_{Pi}} \tag{39}$$

Considering that Eq. (38) must obey Eq. (2), it can be then written as

$$\rho_l(F_p^m - F_P^o)\frac{\Delta V_P}{\Delta t} + \sum \rho_l V_{Pi}\left((\frac{1}{2} - \alpha_i)G_i\right)\Delta S_{Pi} = 0 \tag{40}$$

where the superscript m represents the previous iteration level.

Subtracting Eq. (38) from Eq. (40), one obtains

$$F_P = F_P^m + \frac{\Delta t}{\Delta V_P} G_P \sum \rho_l V_{Pi}\left(\frac{1}{2} + \alpha_i\right)\Delta S_{Pi} \tag{41}$$

which is the equation used to update the liquid fraction field (F).

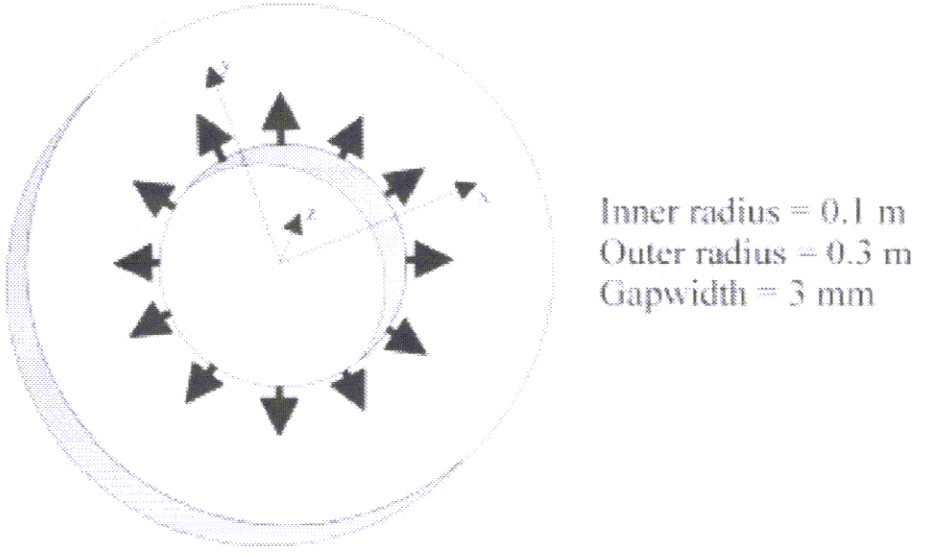

Figure 2. Geometry used to test the methodology

8 SOLUTION PROCEDURE

Following, is a brief description of the numerical procedure:

1. Set or estimate initial values of dependent variables: u, v, w and P. Set also $F = 0$ for all volumes (empty cavity);
2. Calculate de pressure gradient;
3. Calculate de coefficients and source terms for u, v and w. Solve the corresponding linear system, Eq. (18), obtaining u^*, v^* and w^*;
4. Obtain u^*, v^* and w^* at the interfaces;
5. Calculate the coefficients and source term for P'. Solve Eq. (28);
6. Calculate de pressure correction gradient.
7. Velocities u, v and w are corrected using the correcting equations with the pressure correction obtained in item 5.

8. Calculate the new values of F.
9. Return to step 2 until the convergence criteria is achieved, or return to step 2 for the next time step.

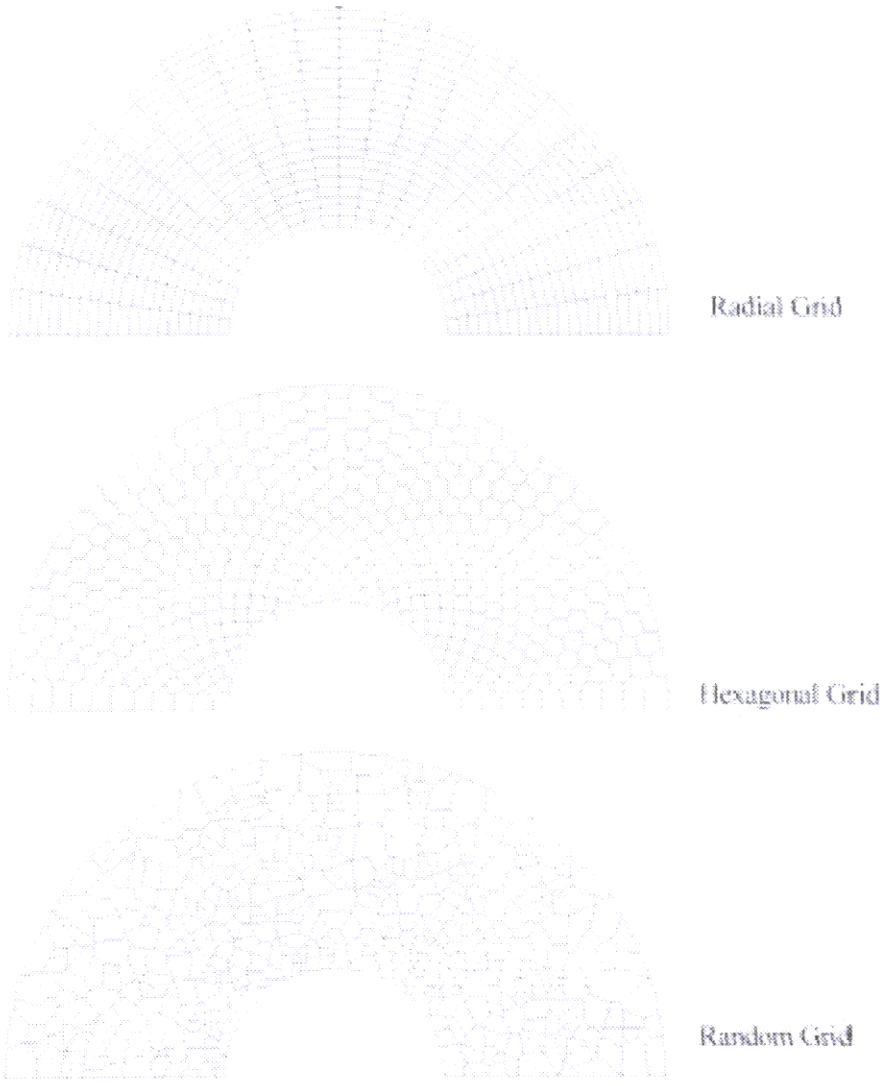

Figure 3. Grids used in radial filling

Table 2 - Results obtained using a 2D numerical model. $R(t)$ in [m].

Time (t) [s]	$R(t)$ Analitical	$R(t)$ Radial	$R(t)$ Hexagonal	$R(t)$ Random
0.001	0.10954	0.10951	0.10951	0.10951
0.002	0.11832	0.11826	0.11826	0.11826
0.003	0.12649	0.12641	0.12641	0.12641
0.004	0.13416	0.13406	0.13406	0.13403
0.005	0.14142	0.14130	0.14130	0.14130
0.006	0.14832	0.14818	0.14818	0.14818
0.007	0.15492	0.15476	0.15476	0.15476
0.008	0.16125	0.16107	0.16107	0.16106
0.009	0.16733	0.16714	0.16714	0.16705
0.010	0.17321	0.17300	0.17300	0.17197
0.011	0.17889	0.17867	0.17867	0.17626
0.012	0.18439	0.18417	0.18418	0.17997

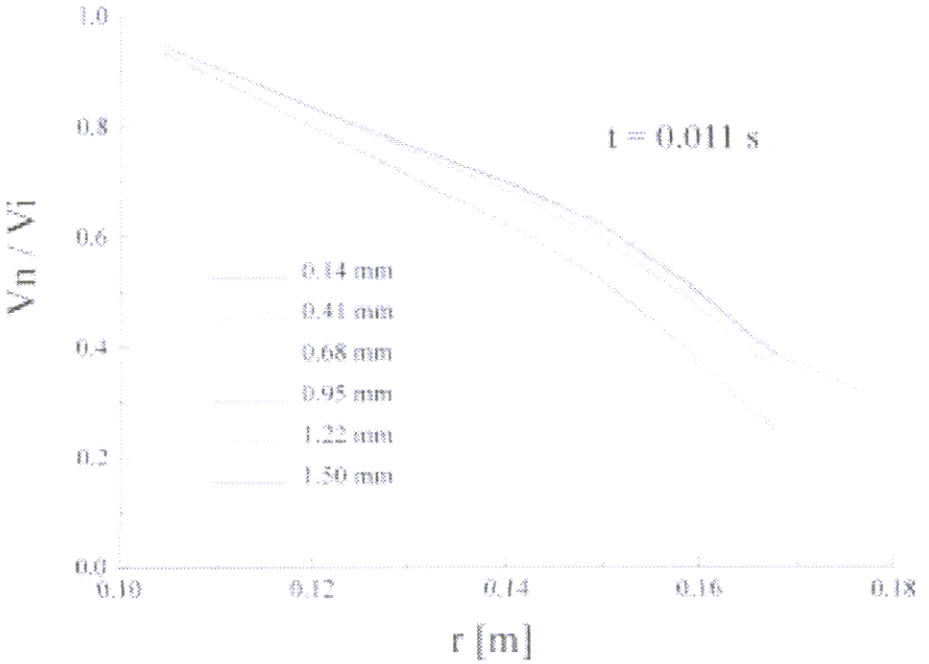

Figure 4. Normal velocity at different z values

9 NUMERICAL RESULTS

The flow injection in a radial cavity offers analytical solution to be compared with the numerical results. This problem is depicted in Fig. 2, where it is shown the dimensions of the cavity. The problem was solved using Voronoi diagrams of polar, hexagonal and random shapes, shown in Fig. 3, in order to evaluate the behavior of the method faced with irregular grid. The problem was solved considering a 2D flow, as usual in this type

of mold filling, and also considering the flow as 3D, for assessing the influences of the velocity in the z-direction. Tables 2 and 3 presents the results for the 2D and the 3D formulation for the three different grids used.

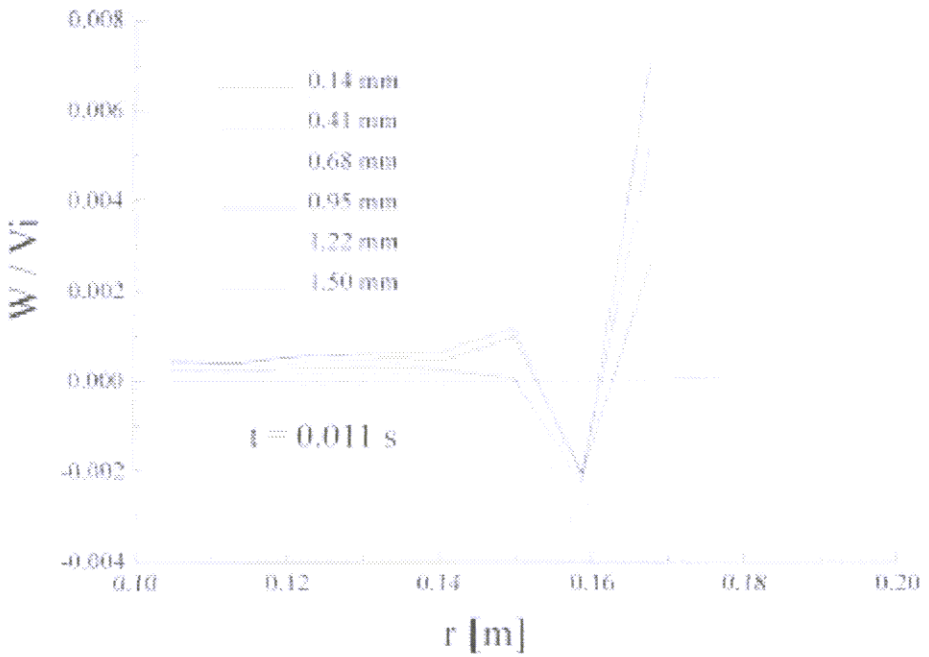

Figure 5. w velocity for different z values

The 2D results were obteined using 484 volumes (radial grids), 473 volumes (hexagonal grids) or 484 volumes (random grids).

Table 3 - Results obtained using a 3D numerical model. $R(t)$ in [m].

Time (t) [s]	$R(t)$ Analitical	$R(t)$ Radial	$R(t)$ Hexagonal	$R(t)$ Random
0.001	0.10954	0.10953	0.10953	0.10953
0.002	0.11832	0.11830	0.11830	0.11830
0.003	0.12649	0.12641	0.12641	0.12647
0.004	0.13416	0.13406	0.13406	0.13413
0.005	0.14142	0.14139	0.14139	0.14139
0.006	0.14832	0.14829	0.14829	0.14829
0.007	0.15492	0.15488	0.15488	0.15488
0.008	0.16125	0.16120	0.16120	0.16120
0.009	0.16733	0.16728	0.16728	0.16729
0.010	0.17321	0.17315	0.17315	0.17316
0.011	0.17889	0.17883	0.17883	0.17873
0.012	0.18439	0.18433	0.18443	0.17382

For all problems showed in this work $\rho_g = 0.35$ kg/m^3, $\rho_l = 2500$ kg/m^3, $\mu_g = 4.0 \times 10^{-5}$ kg/m/s and $\mu_l = 2.5 \times 10^{-3}$ kg/m/s.

The 3D results were obtained using 5,324 volumes (radial grid), 5,203 volumes (hexagonal grid) or 5,324 volumes (random grid). There were 11 volumes in the z-direction for all cases.

The analytical results presented in Tables 2 and 3 is the solution of the the following equation

$$\frac{\partial}{\partial r}\left[\mu r \frac{\partial P}{\partial r}\right] = 0 \qquad \text{with} \qquad \begin{array}{lll} r = R_o & \text{then} & V = V_i \\ r = R(t) & \text{then} & P = 0 \end{array} \tag{42}$$

which gives the radial position, $R(t)$, of the filling front,

$$R(t) = \sqrt{2V_i R_o t + R_o^2} \tag{43}$$

where R_o is the inner radius, V_i is the constant fluid velocity in R_o and t is the time. Using the numerical results, the radial position is calculated by

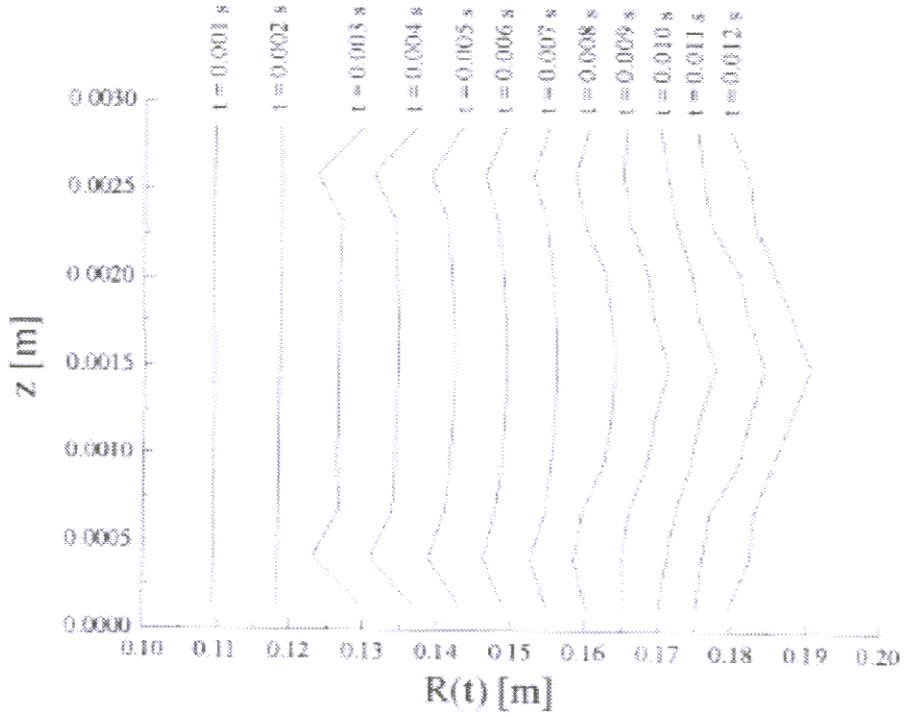

Figure 6. Front position at different times

$$R(t) = \sqrt{\frac{2A_i}{\pi \Delta h} + R_o^2} \tag{44}$$